

Supporting Information

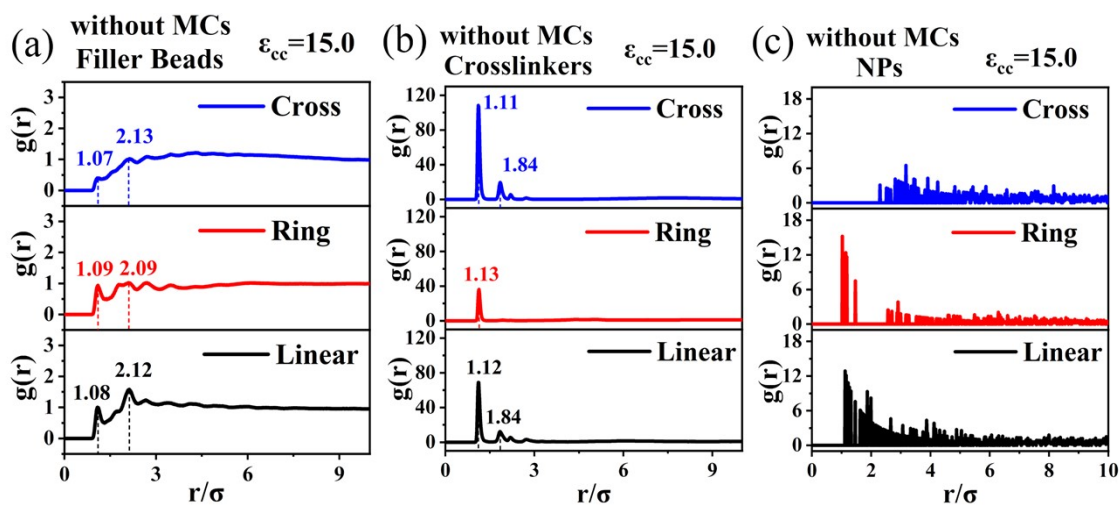


Figure S1. In configurations without MCs. (a) The RDF of filler beads at $\epsilon_{cc} = 15.0$, (b) the RDF of Crosslinkers at $\epsilon_{cc} = 15.0$ and (c) the RDF of whole NPs at $\epsilon_{cc} = 15.0$.

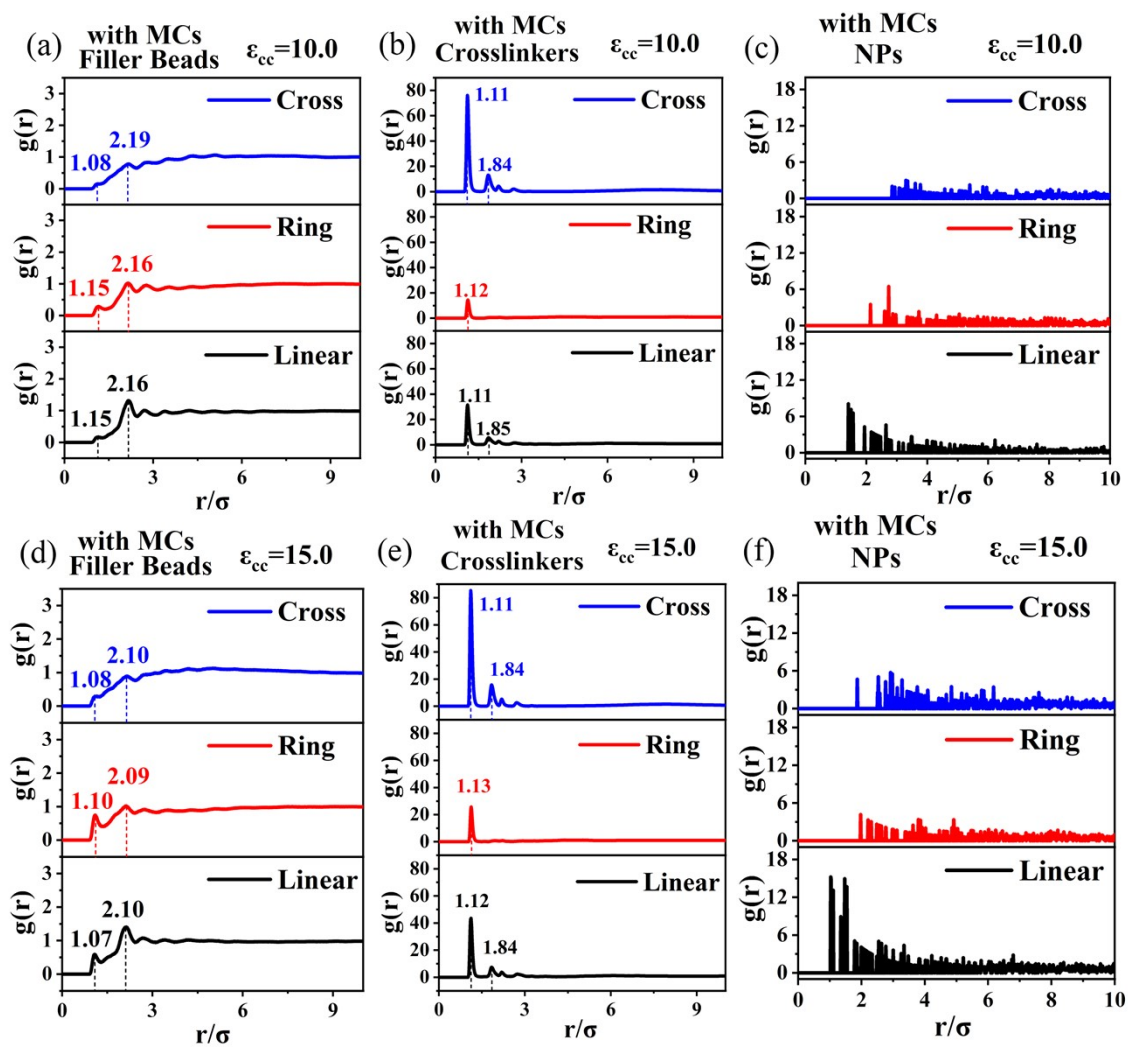


Figure S2. In configurations with MCs. The RDF of (a) filler beads, (b) Crosslinkers and (c) whole NPs at $\epsilon_{cc} = 10.0$.

The RDF of (d) filler beads, (e) Crosslinkers and (f) whole NPs at $\epsilon_{cc} = 15.0$.

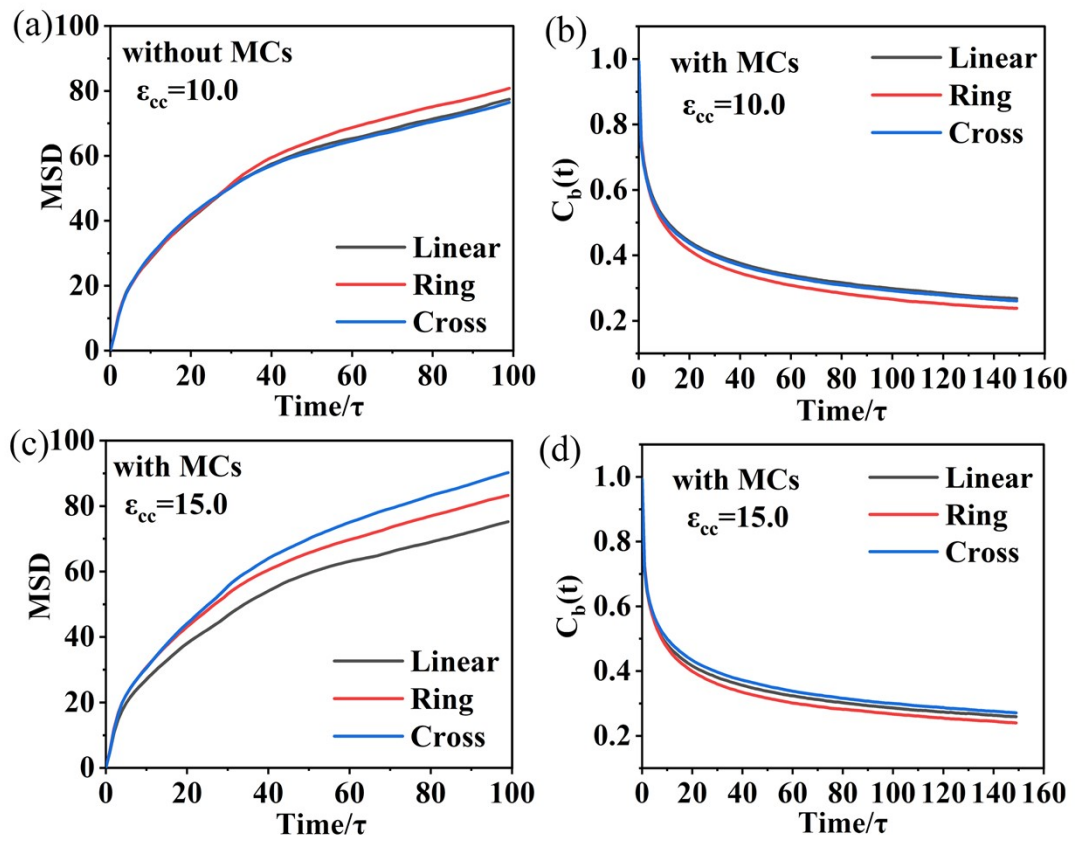


Figure S3. In configuration with MCs, the (a) MSD and (b) the bond autocorrelation function at $\epsilon_{cc} = 10.0$. The (c) MSD and (d) the bond autocorrelation function at $\epsilon_{cc} = 15.0$.

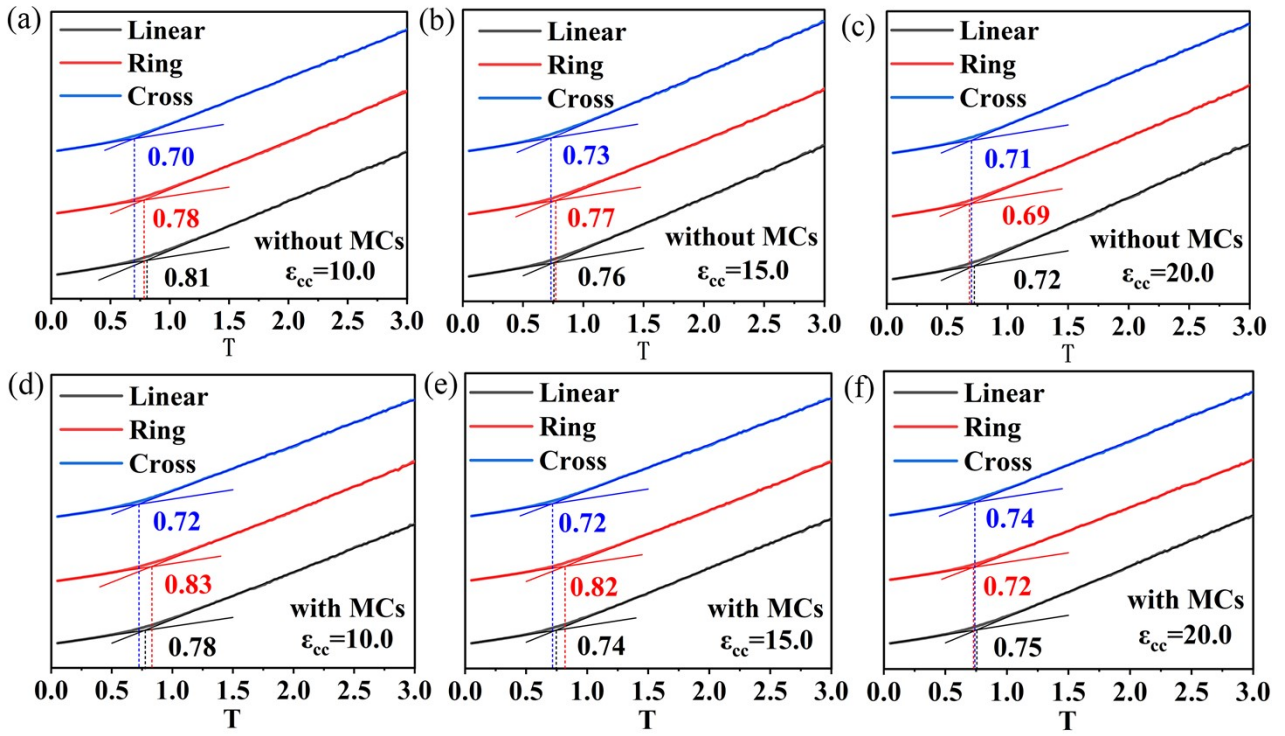


Figure S4. The fitting curves of the function about the volume and temperature: (a) without MCs at $\epsilon_{cc} = 10.0$, (b) without MCs at $\epsilon_{cc} = 15.0$, (c) without MCs at $\epsilon_{cc} = 20.0$ and (d) with MCs at $\epsilon_{cc} = 10.0$, (e) with MCs at $\epsilon_{cc} = 15.0$, (f) with MCs at $\epsilon_{cc} = 20.0$.

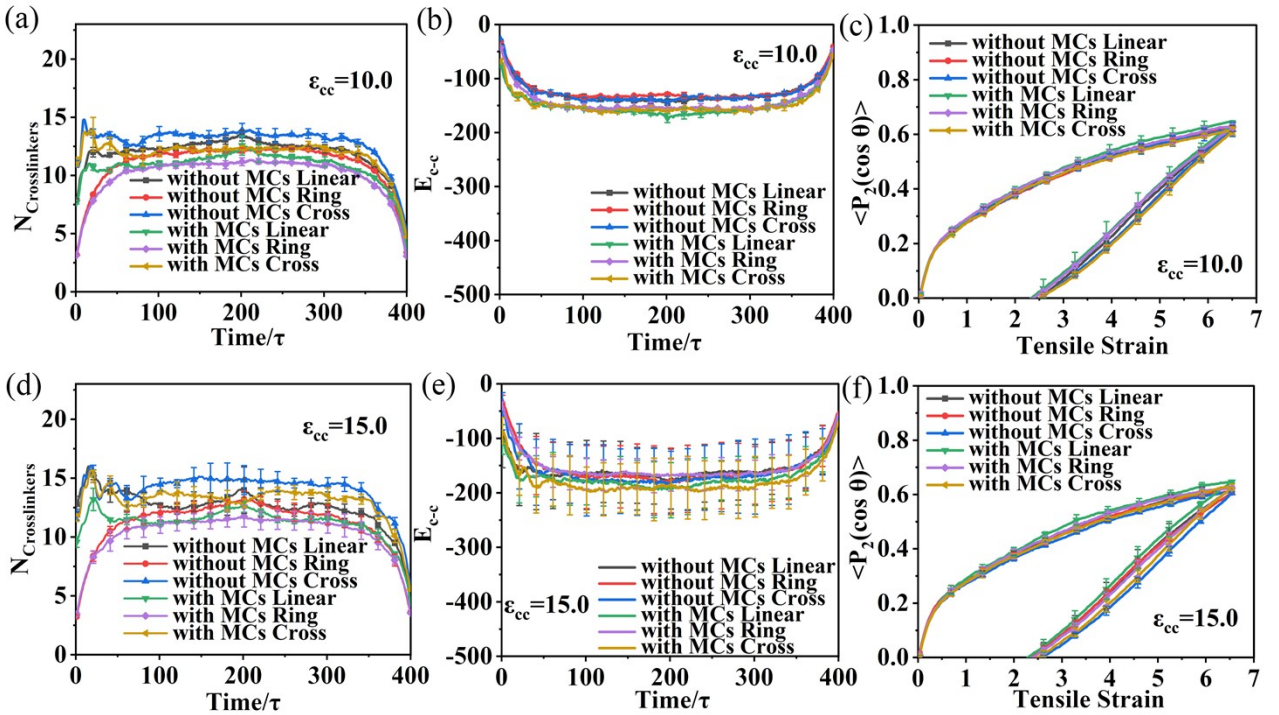


Figure S5. During the uniaxial tension and recovery process. (a) The average number of neighbor Crosslinkers, (b) the total interaction energy between Crosslinkers and (c) the matrix chains orientation at $\epsilon_{cc} = 10.0$. (d) The average number of neighbor Crosslinkers, (e) the total interaction energy between Crosslinkers and (f) the matrix chains orientation at $\epsilon_{cc} = 15.0$.

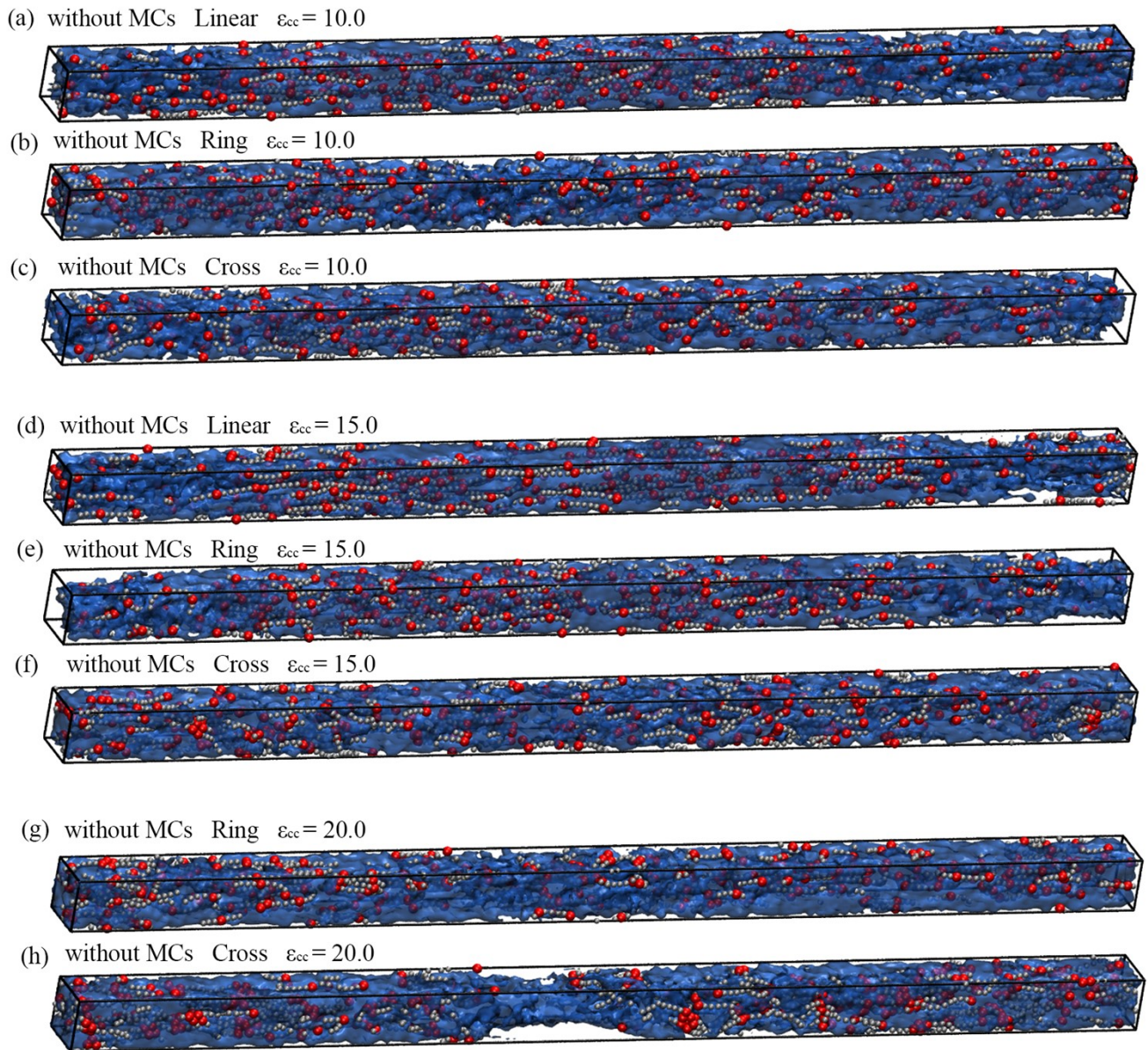
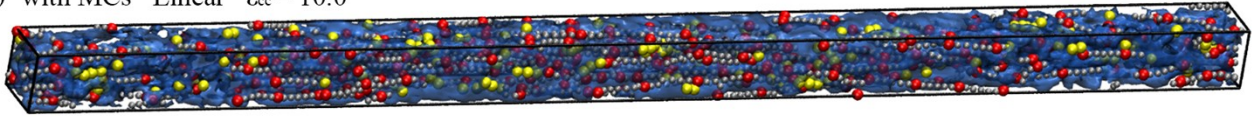
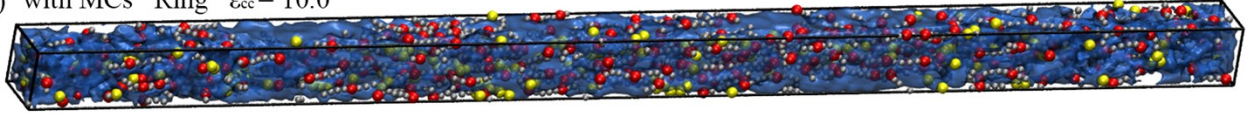


Figure S6. The snapshots at maximum uniaxial strain of (a) Linear, (b) Ring and (c) Cross structure PNCs without MCs at $\epsilon_{cc} = 10.0$. (d) Linear, (e) Ring and (f) Cross structure PNCs without MCs at $\epsilon_{cc} = 15.0$. (g) Ring and (h) Cross structure PNCs without MCs at $\epsilon_{cc} = 20.0$.

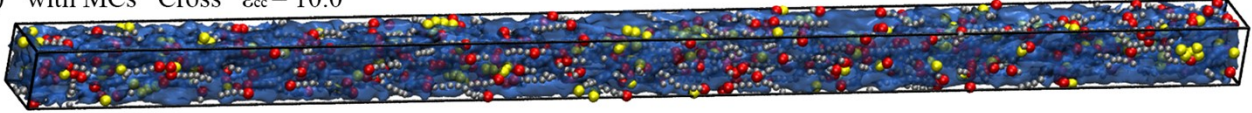
(a) with MCs Linear $\epsilon_{cc} = 10.0$



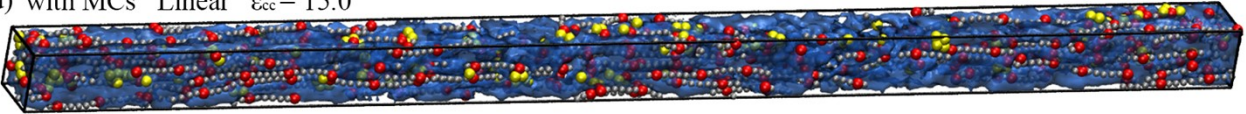
(b) with MCs Ring $\epsilon_{cc} = 10.0$



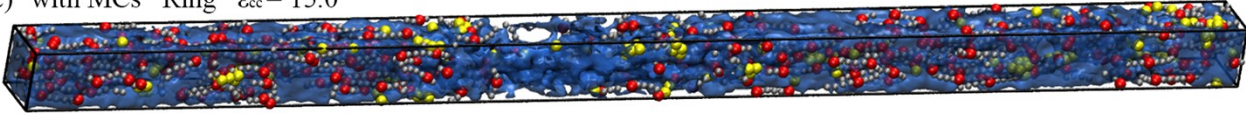
(c) with MCs Cross $\epsilon_{cc} = 10.0$



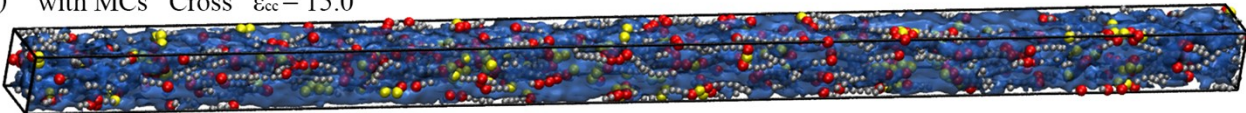
(d) with MCs Linear $\epsilon_{cc} = 15.0$



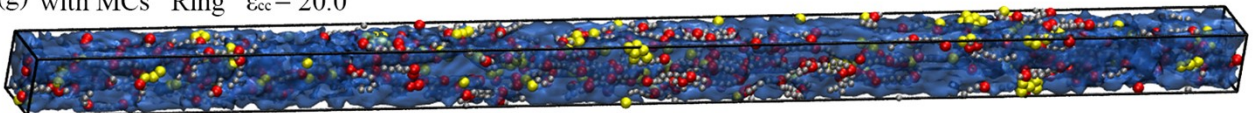
(e) with MCs Ring $\epsilon_{cc} = 15.0$



(f) with MCs Cross $\epsilon_{cc} = 15.0$



(g) with MCs Ring $\epsilon_{cc} = 20.0$



(h) with MCs Cross $\epsilon_{cc} = 20.0$

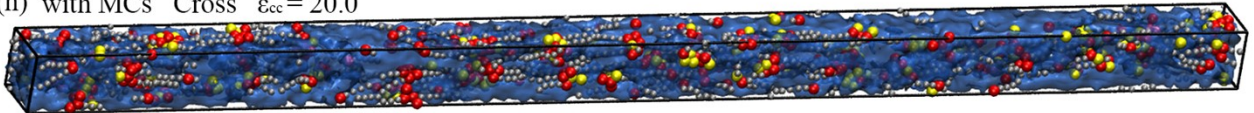


Figure S7. The snapshots at maximum uniaxial strain of (a) Linear, (b) Ring and (c) Cross structure PNCs with MCs at $\epsilon_{cc} = 10.0$. (d) Linear, (e) Ring and (f) Cross structure PNCs with MCs at $\epsilon_{cc} = 15.0$. (g) Ring and (h) Cross structure PNCs with MCs at $\epsilon_{cc} = 20.0$.

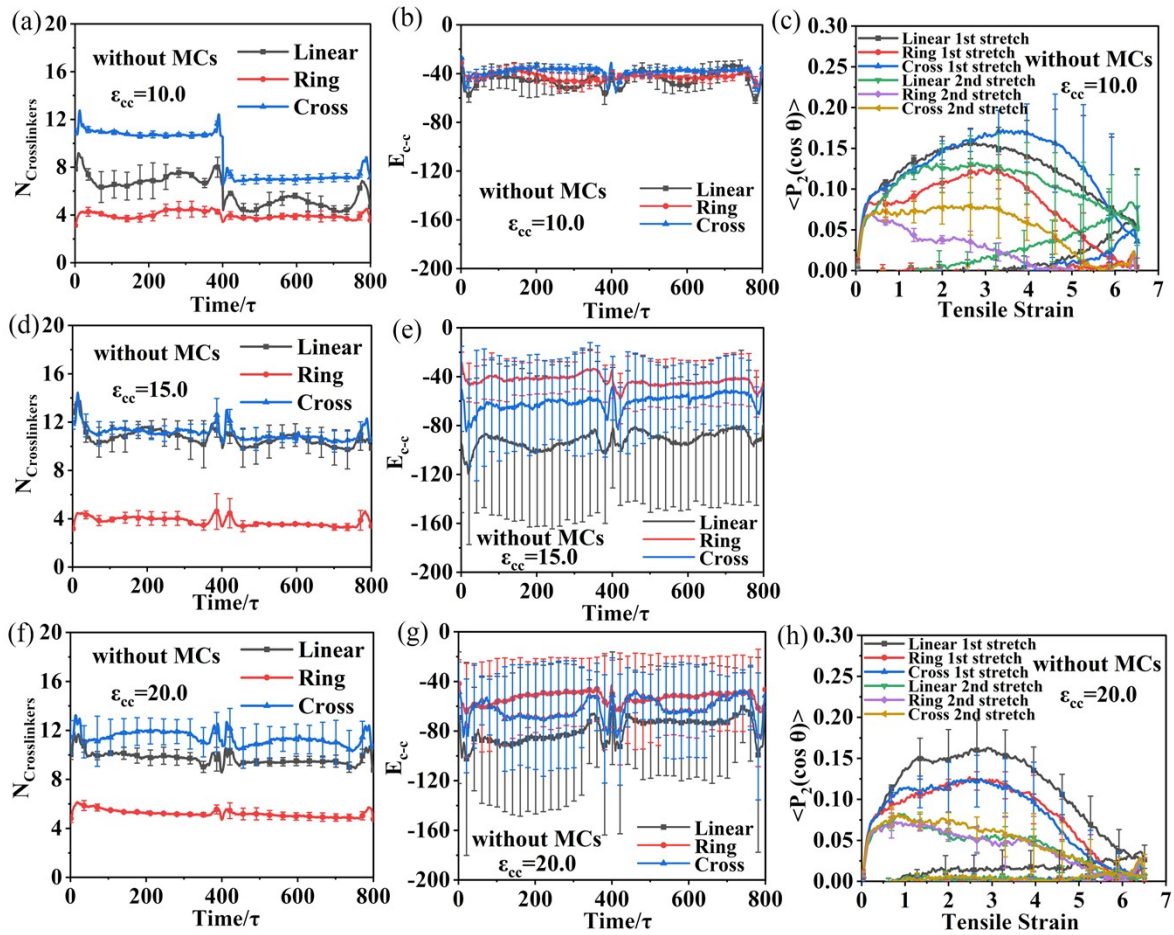
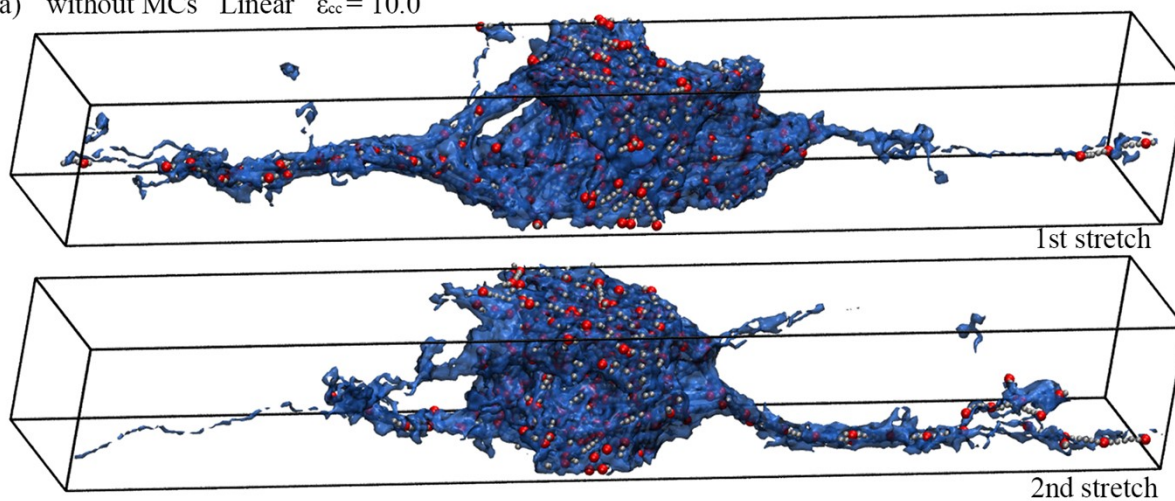
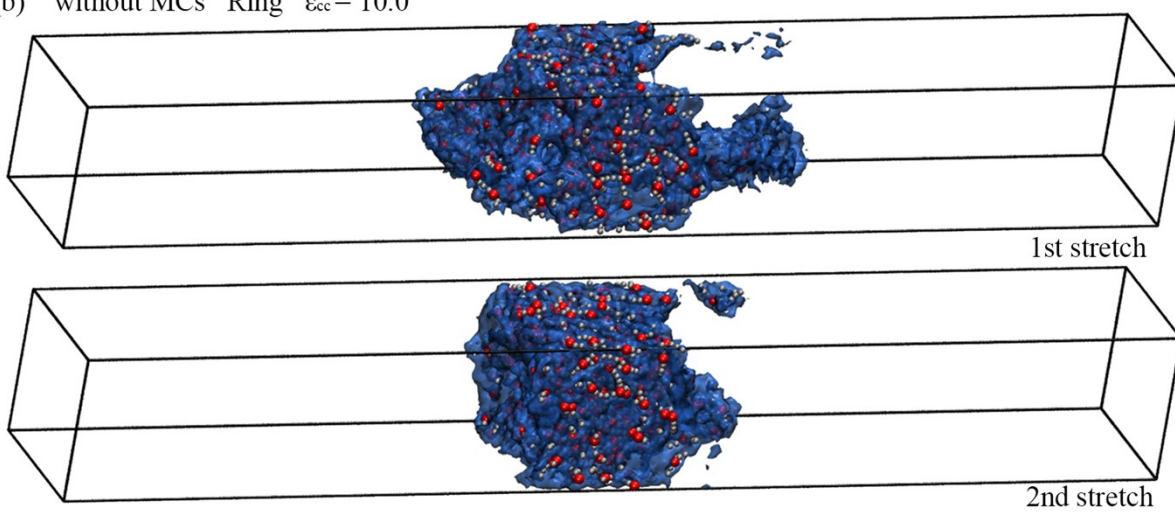


Figure S8. In the configurations without MCs, during the twice approximate triaxial tension and recovery process. (a) The average number of neighbor Crosslinkers, (b) total interaction energy between Crosslinkers and (c) the matrix chains orientation at $\epsilon_{cc} = 10.0$. (d) The average number of neighbor Crosslinkers and (e) total interaction energy between Crosslinkers $\epsilon_{cc} = 15.0$. (f) The average number of neighbor Crosslinkers, (g) total interaction energy between Crosslinkers and (h) the matrix chains orientation at $\epsilon_{cc} = 20.0$.

(a) without MCs Linear $\epsilon_{cc} = 10.0$



(b) without MCs Ring $\epsilon_{cc} = 10.0$



(c) without MCs Cross $\epsilon_{cc} = 10.0$

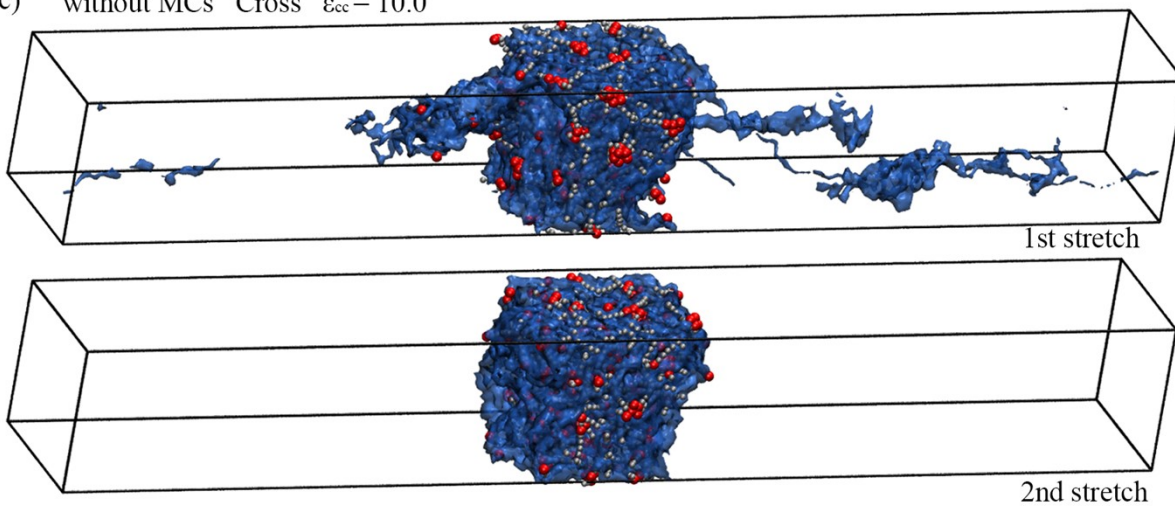
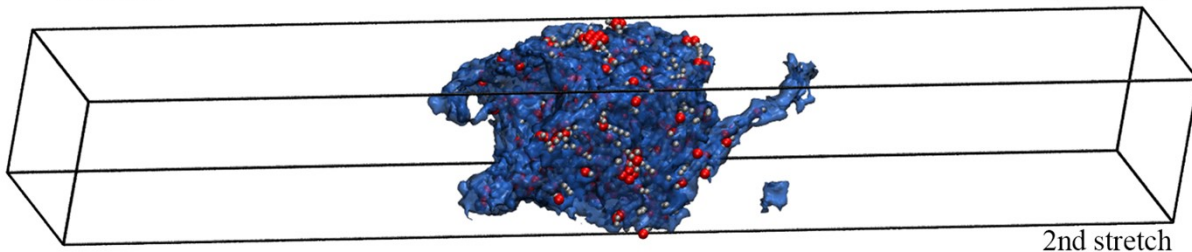
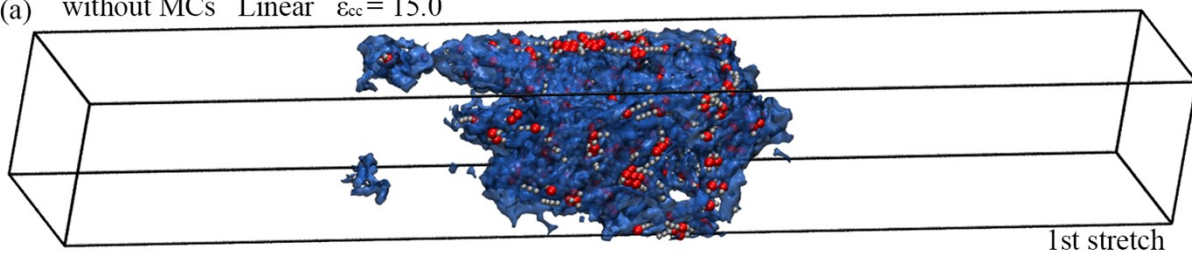


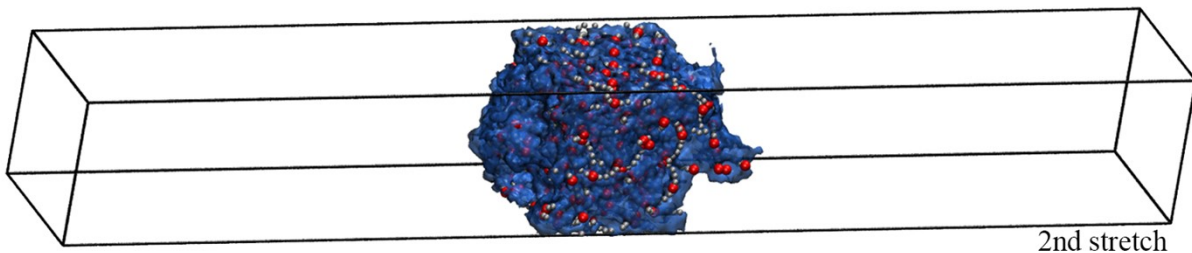
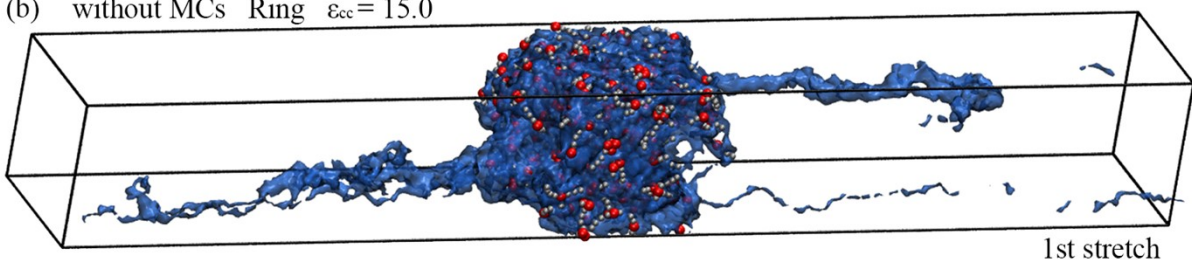
Figure S9. In the configurations without MCs. The snapshots at maximum strain of (a) Linear, (b) Ring and (c)

Cross structure PNCs at $\epsilon_{cc} = 10.0$ in approximate triaxial tension and recovery process.

(a) without MCs Linear $\epsilon_{cc} = 15.0$



(b) without MCs Ring $\epsilon_{cc} = 15.0$



(c) without MCs Cross $\epsilon_{cc} = 15.0$

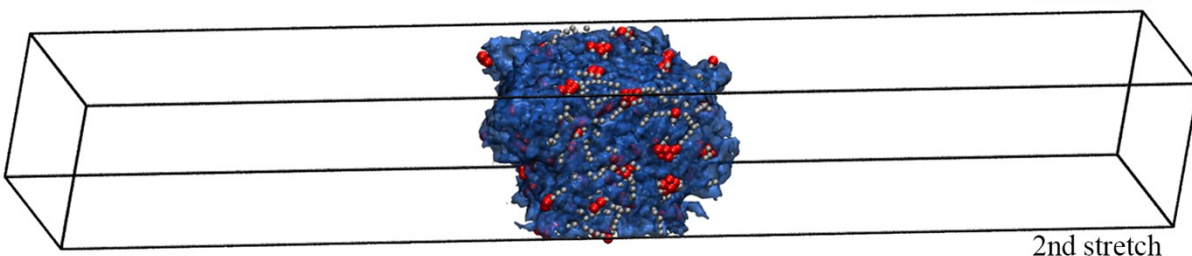
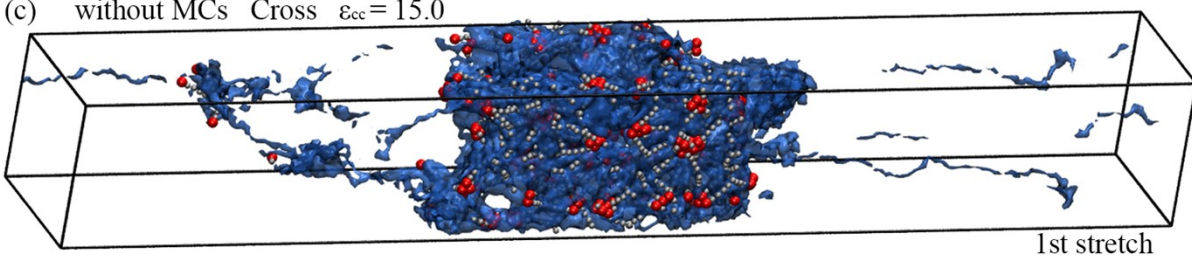
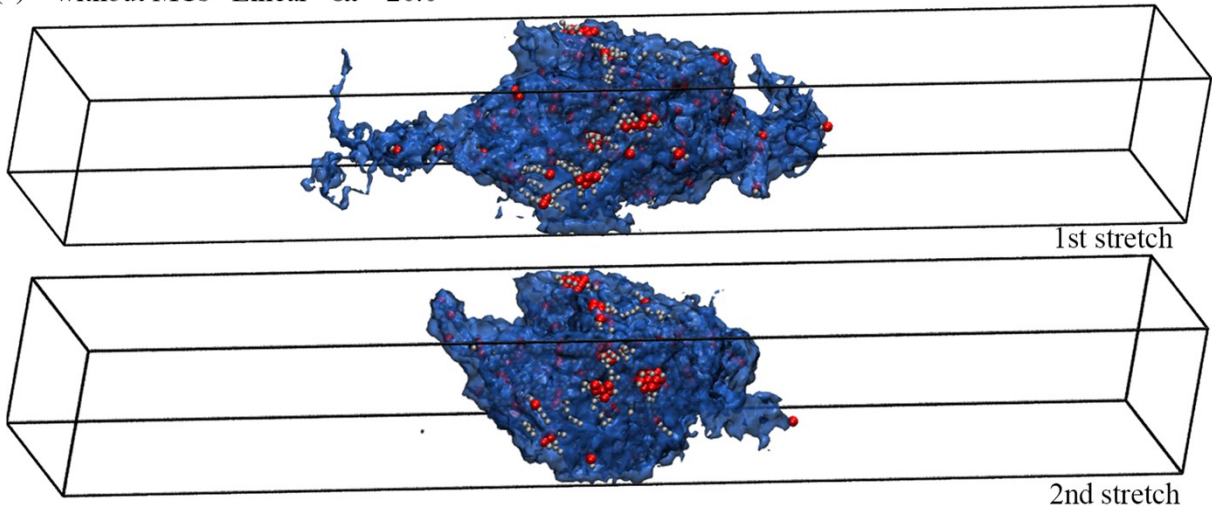


Figure S10. In the configurations without MCs. The snapshots at maximum strain of (a) Linear, (b) Ring and (c)

Cross structure PNCs at $\varepsilon_{cc} = 15.0$ in approximate triaxial tension and recovery process.

(a) without MCs Linear $\varepsilon_{cc} = 20.0$



(b) without MCs Cross $\varepsilon_{cc} = 20.0$

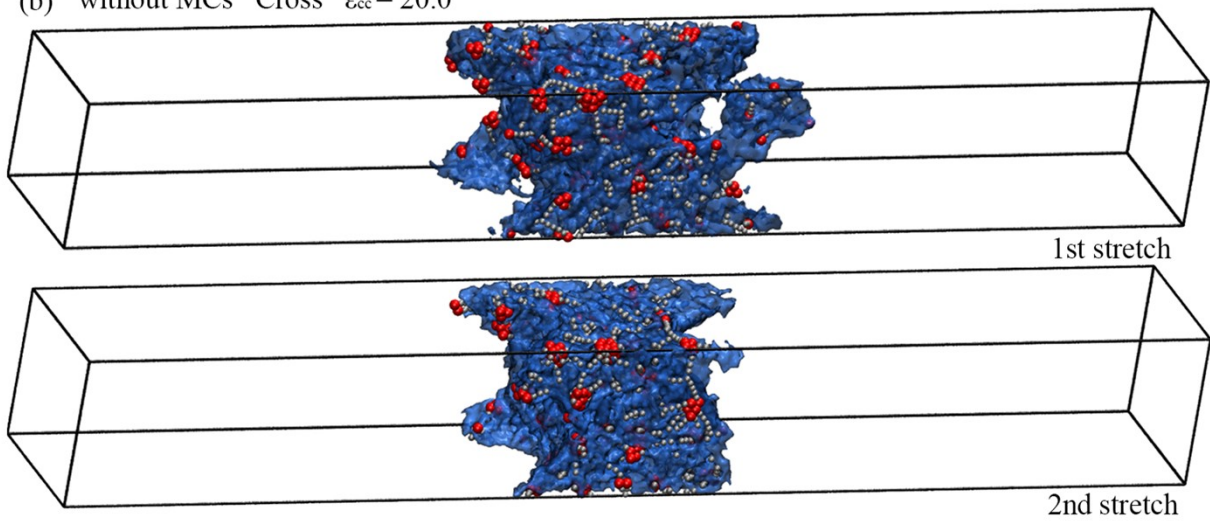


Figure S11. In the configurations without MCs. The snapshots at maximum strain of (a) Linear and (b) Cross

structure PNCs at $\varepsilon_{cc} = 20.0$ during approximate triaxial tension and recovery process.

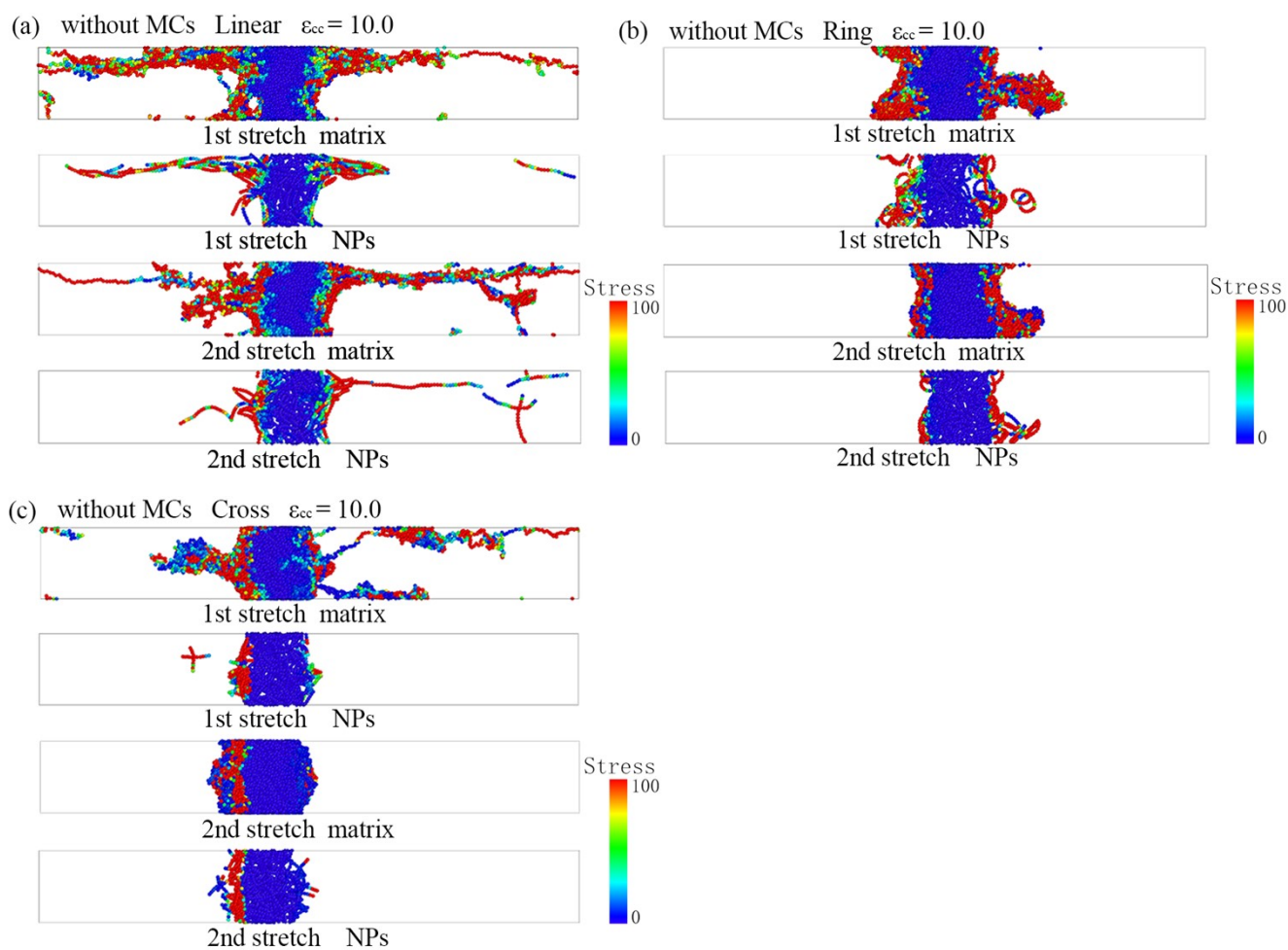


Figure S12. In the configurations without MCs. The heatmaps of matrix and NPs of (a) Linear, (b) Ring and (c) Cross structure PNCs at $\epsilon_{cc} = 10.0$ during approximate triaxial tension and recovery process when stretched to maximum strain.

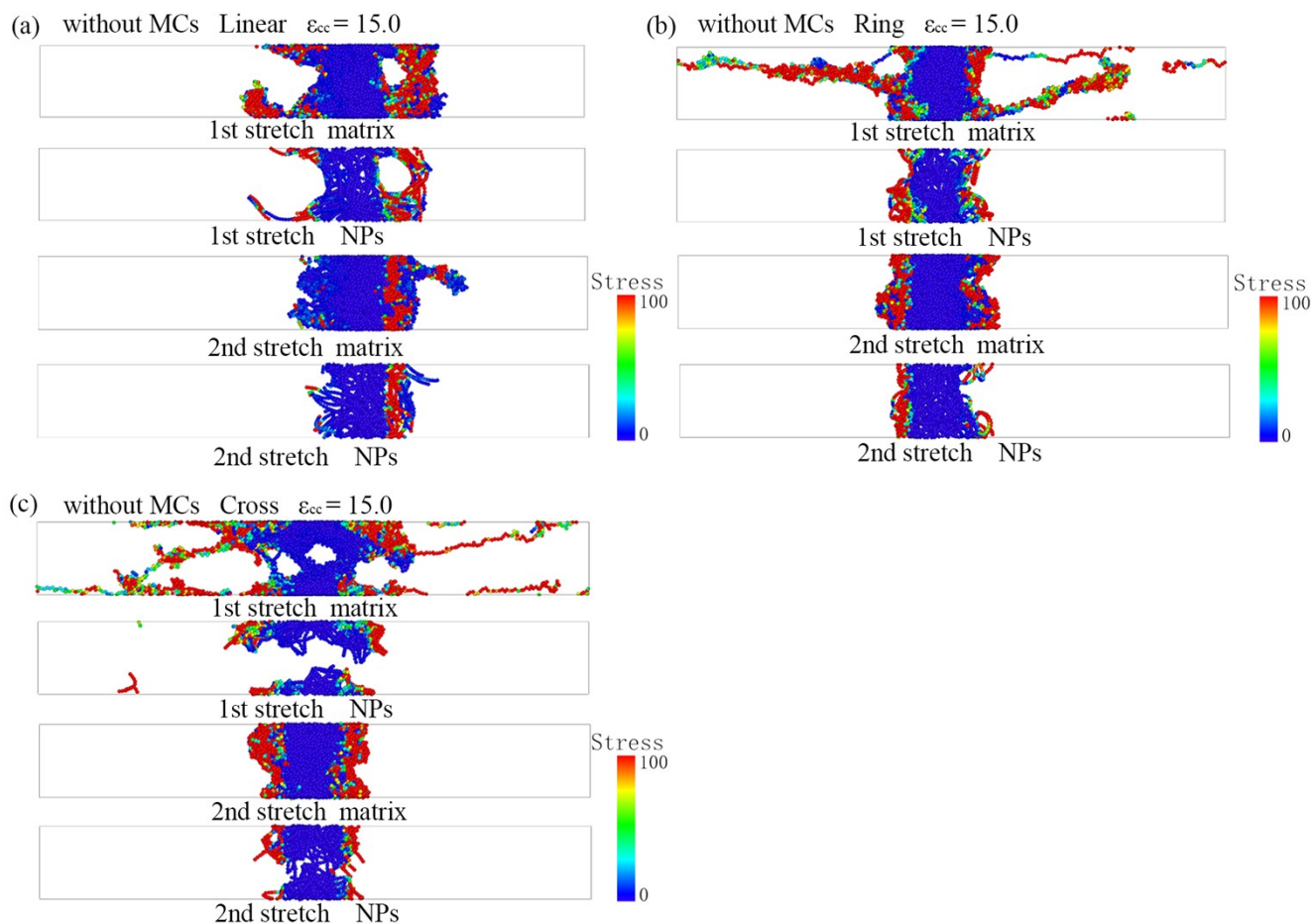


Figure S13. In the configurations without MCs. The heatmaps of matrix and NPs of (a) Linear, (b) Ring and (c) Cross structure PNCs at $\epsilon_{cc} = 15.0$ during approximate triaxial tension and recovery process when stretched to maximum strain.

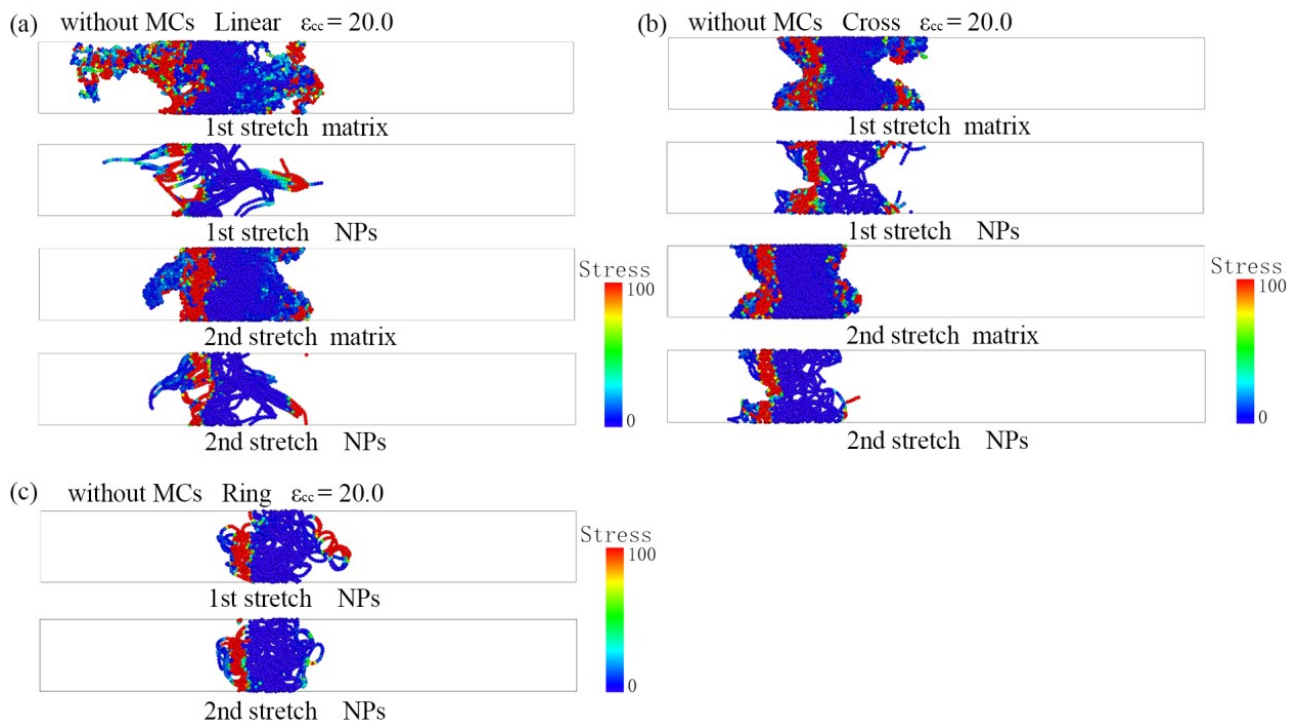


Figure S14. In the configurations without MCs. The heatmaps of matrix and NPs of (a) Linear and (b) Cross structure PNCs at $\epsilon_{cc} = 20.0$, and (c) the heatmaps of NPs of Ring structure PNCs at $\epsilon_{cc} = 20.0$ during approximate triaxial tension and recovery process when stretched to maximum strain.

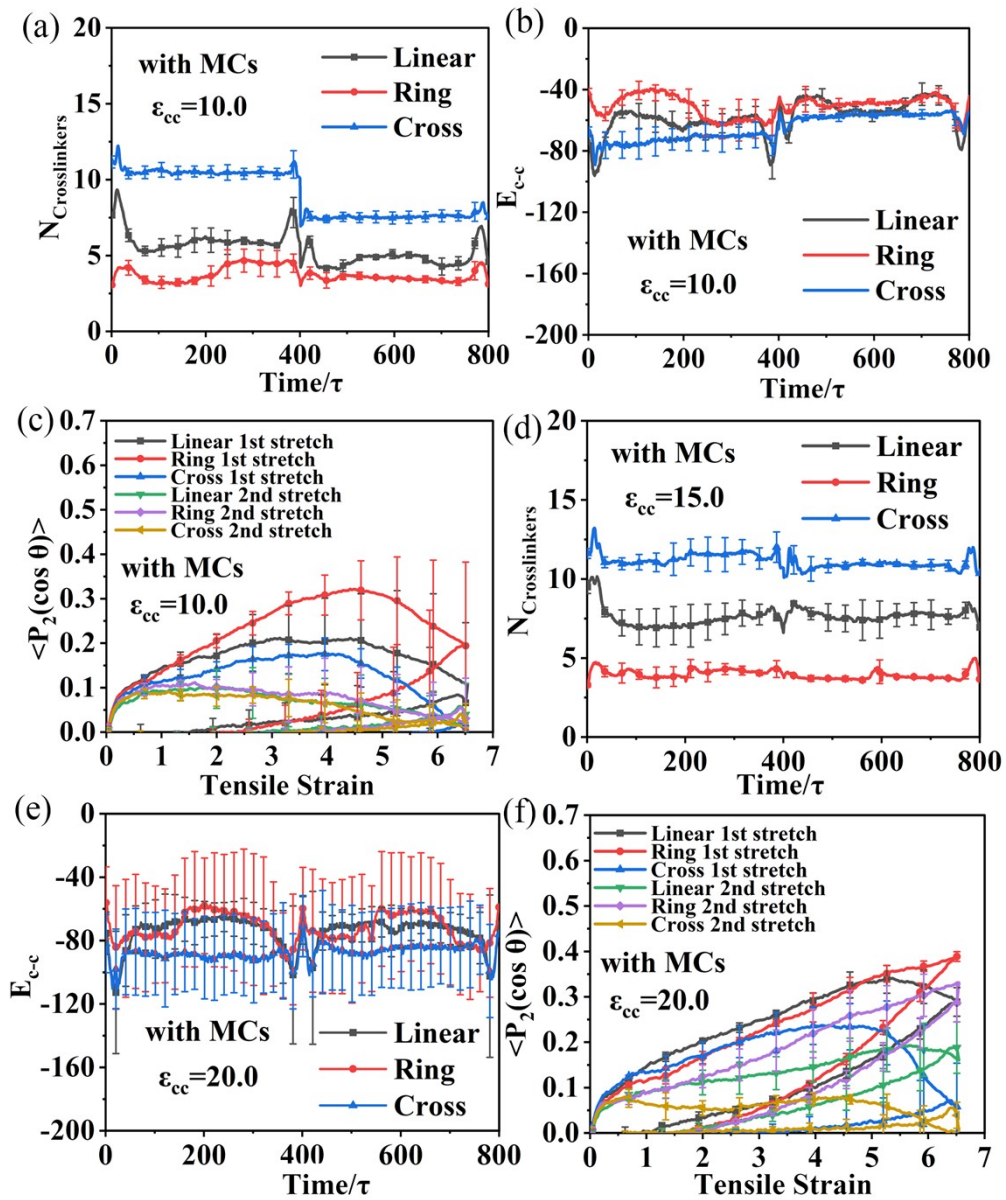


Figure S15. In the configurations with MCs, during the twice approximate triaxial tension and recovery process.

(a) The average number of neighbor Crosslinkers, (b) total interaction energy between Crosslinkers and (c) the matrix chains orientation at $\epsilon_{cc} = 10.0$. (d) The average number of neighbor Crosslinkers at $\epsilon_{cc} = 15.0$. (e) The total interaction energy between Crosslinkers and (f) the matrix chains orientation at $\epsilon_{cc} = 20.0$.

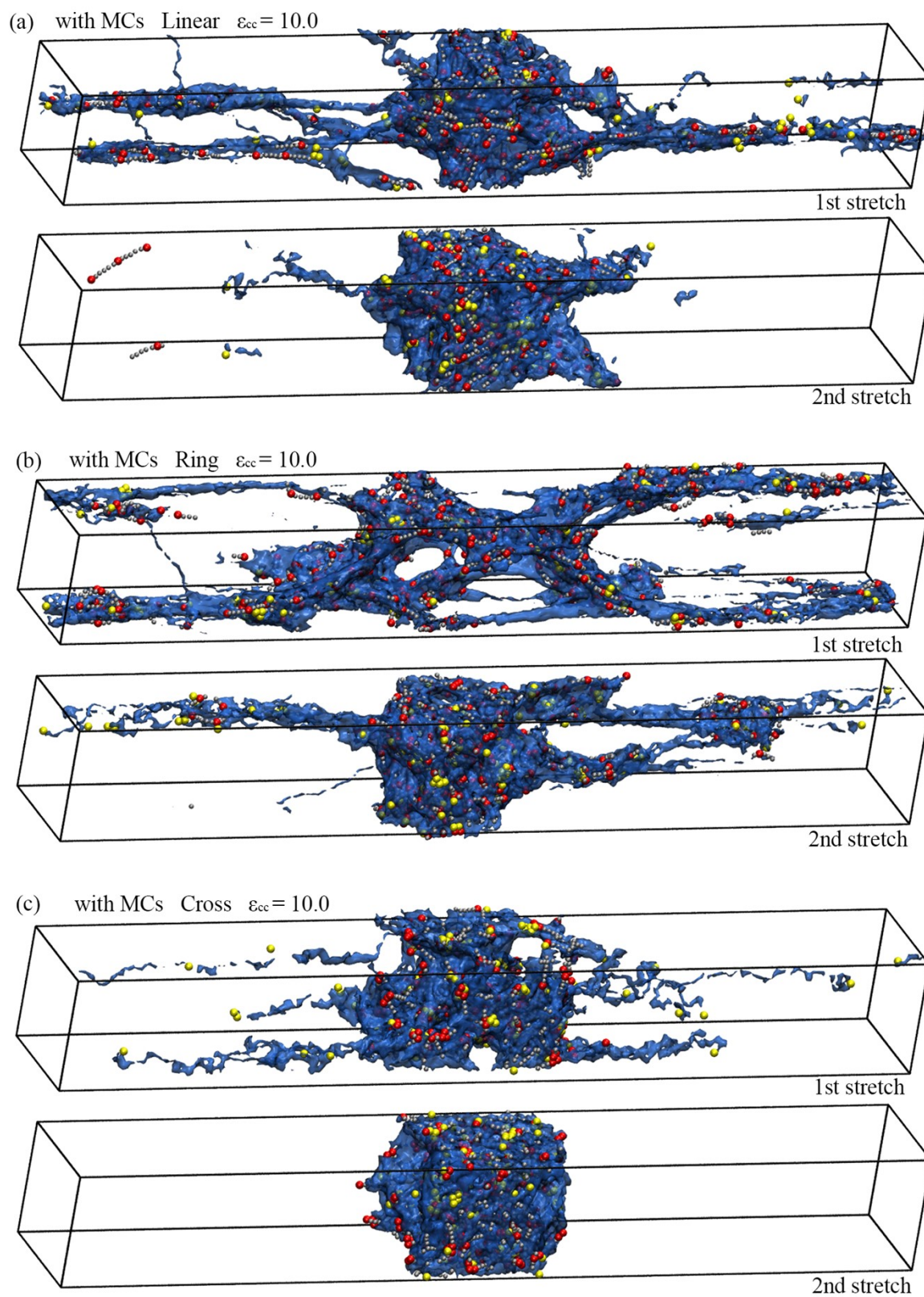
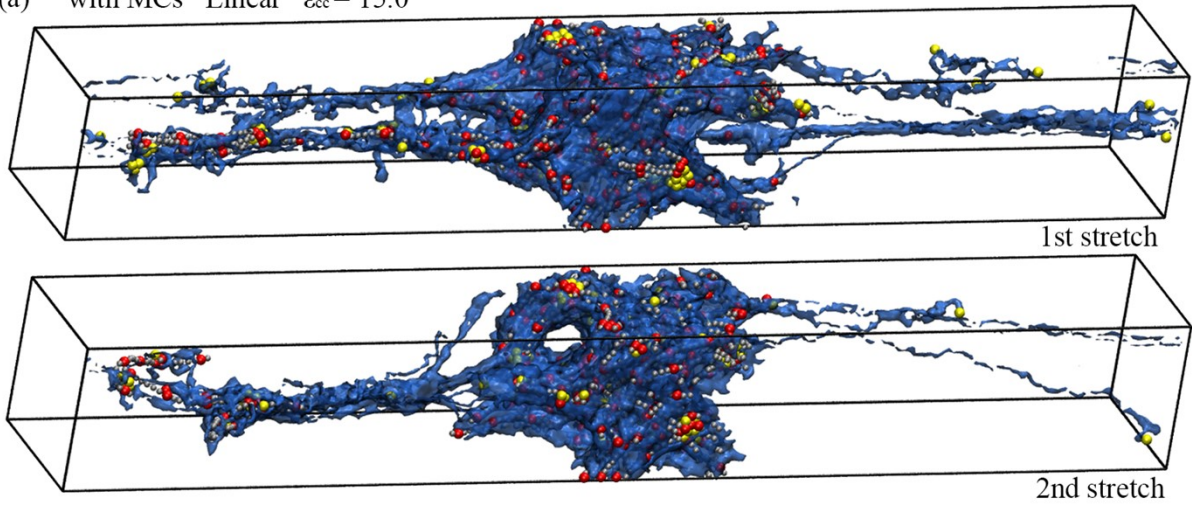


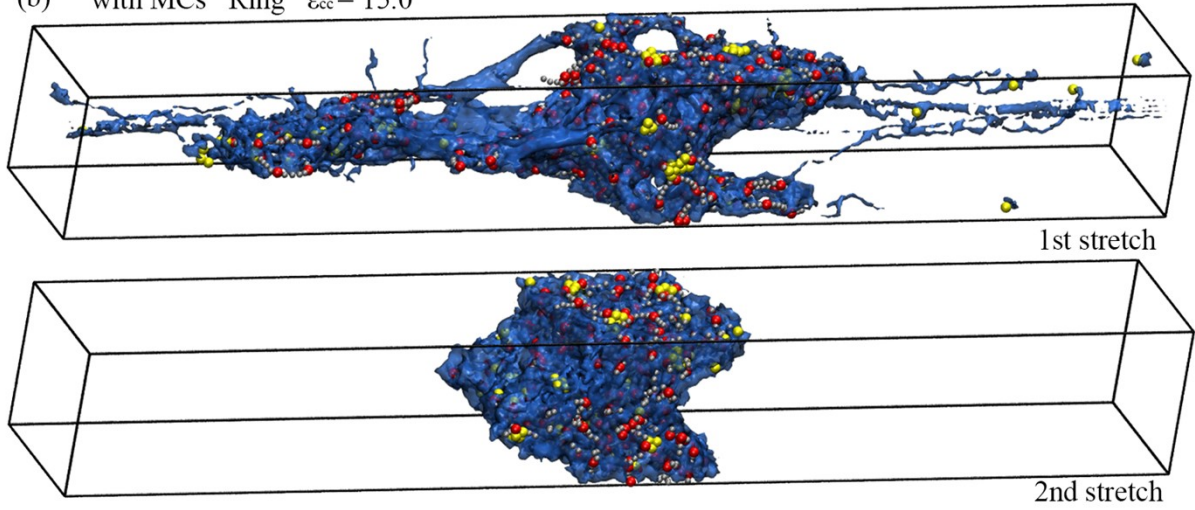
Figure S16. In the configurations with MCs. The snapshots at maximum strain of (a) Linear, (b) Ring and (c)

Cross structure PNCs at $\epsilon_{cc} = 10.0$ during approximate triaxial tension and recovery process.

(a) with MCs Linear $\epsilon_{cc} = 15.0$



(b) with MCs Ring $\epsilon_{cc} = 15.0$



(c) with MCs Cross $\epsilon_{cc} = 15.0$

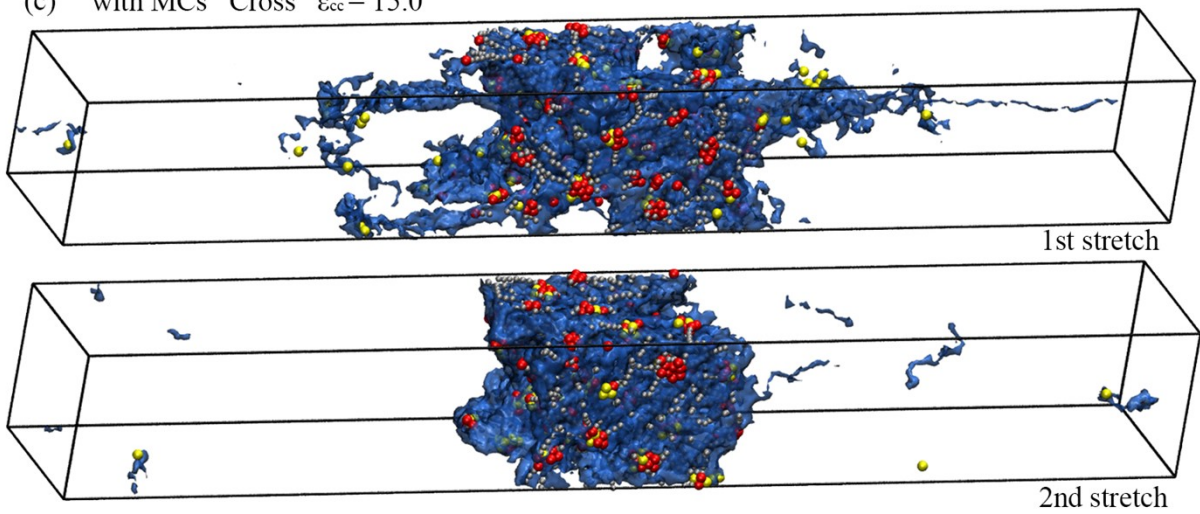


Figure S17. In the configurations with MCs. The snapshots at maximum strain of (a) Linear, (b) Ring and (c) Cross structure PNCs at $\epsilon_{cc} = 15.0$ during approximate triaxial tension and recovery process.

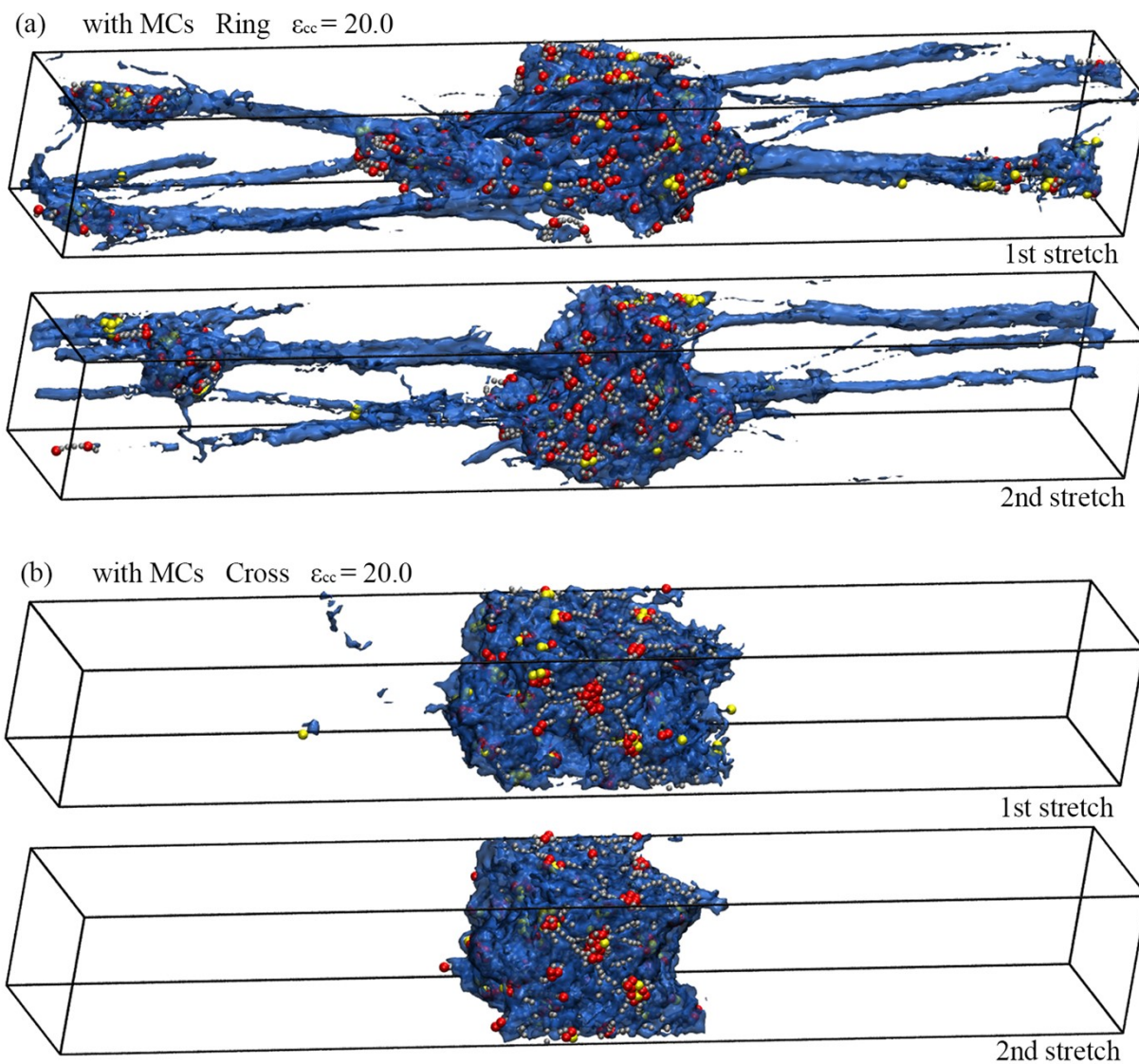


Figure S18. In the configurations with MCs. The snapshots at maximum strain of (a) Ring and (b) Cross structure PNCs at $\epsilon_{cc} = 20.0$ during approximate triaxial tension and recovery process.

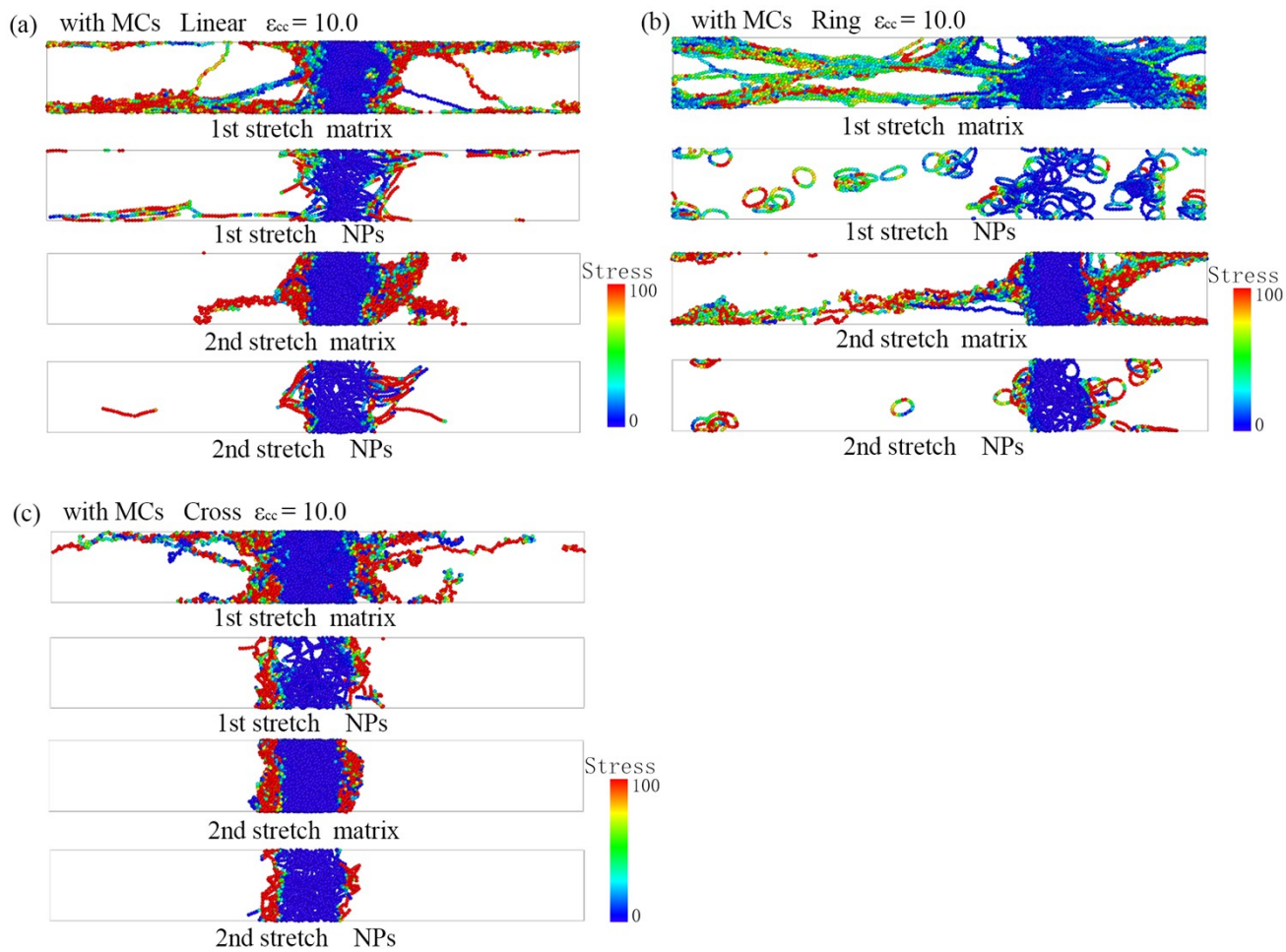


Figure S19. In the configurations with MCs. The heatmaps of matrix and NPs of (a) Linear, (b) Ring and (c) Cross structure PNCs at $\epsilon_{cc} = 10.0$ during approximate triaxial tension and recovery process when stretched to maximum strain.

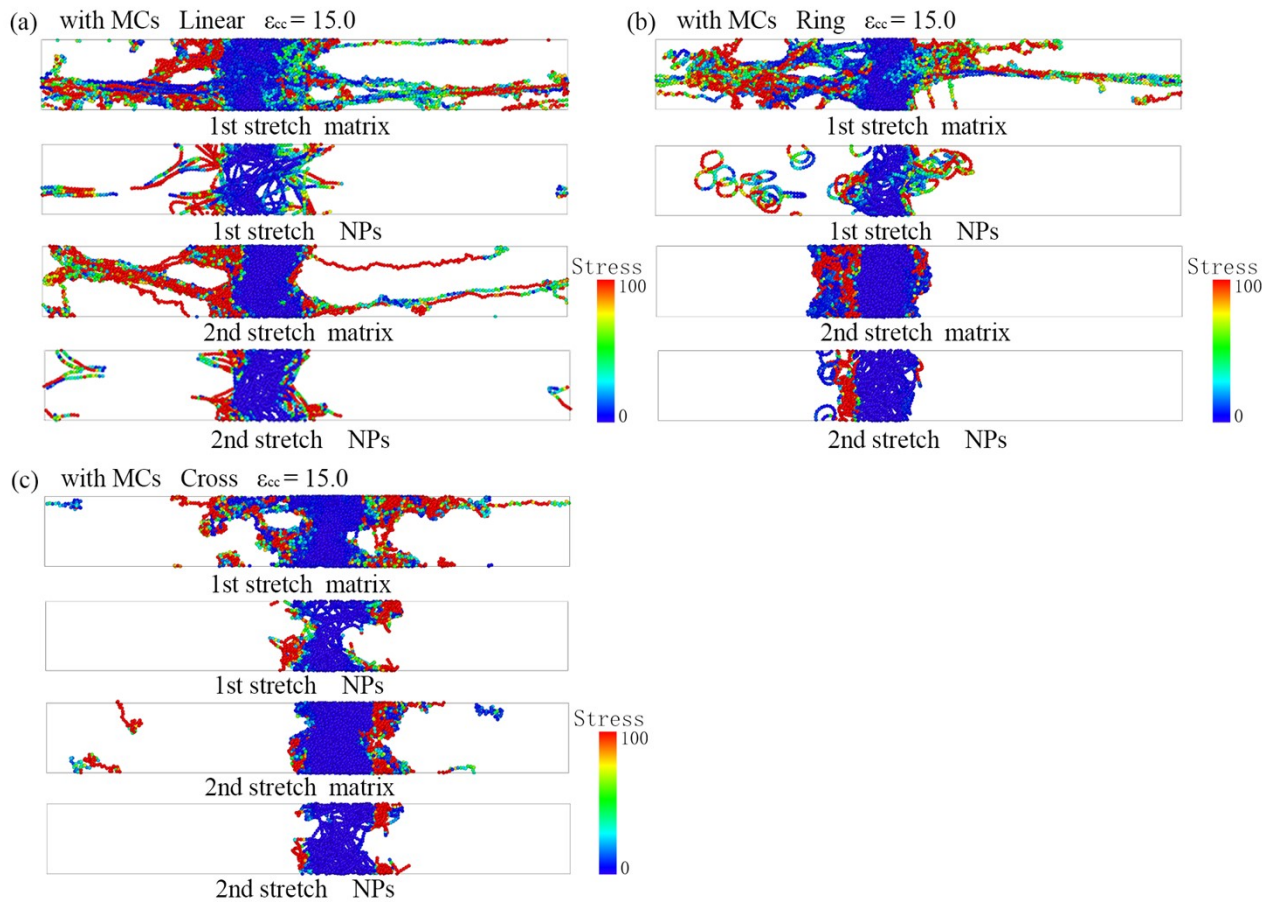


Figure S20. In the configurations with MCs. The heatmaps of matrix and NPs of (a) Linear, (b) Ring and (c) Cross structure PNCs at $\epsilon_{cc} = 15.0$ during approximate triaxial tension and recovery process when stretched to maximum strain.

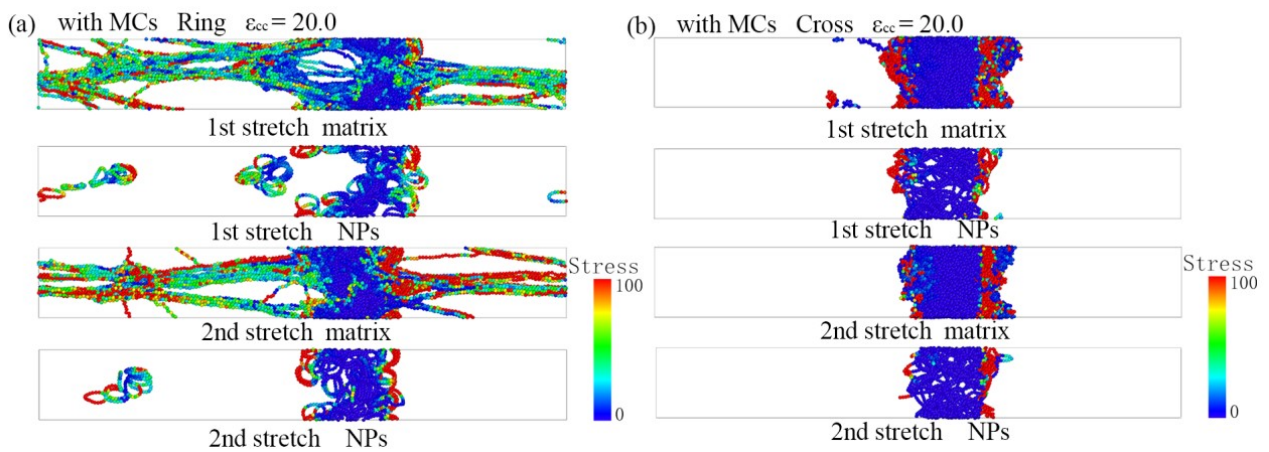


Figure S21. In the configurations with MCs. The heatmaps of matrix and NPs of (a) Ring and (b) Cross structure PNCs at $\epsilon_{cc} = 20.0$ during approximate triaxial tension and recovery process when stretched to maximum strain.

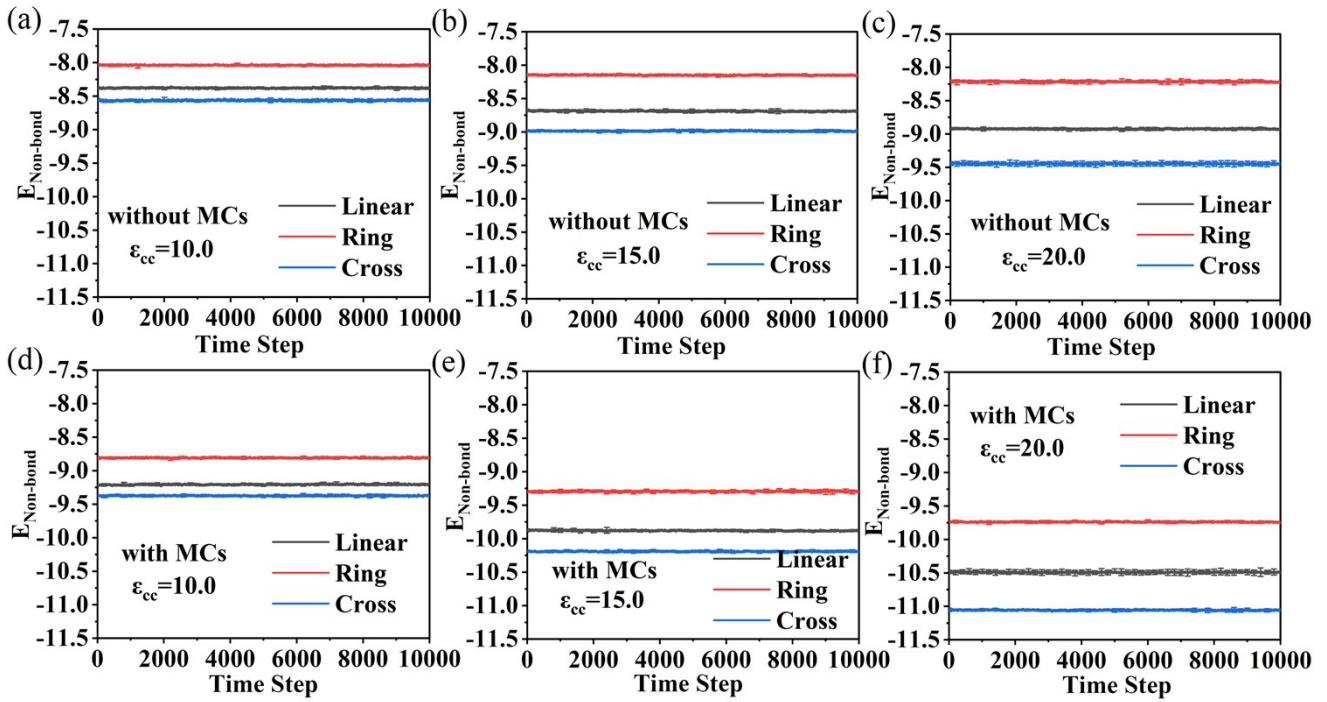


Figure S22. The last 10,000 steps of the equilibrium process of non-bond interaction energy curve: configurations without MCs at (a) $\epsilon_{cc} = 10.0$, (b) $\epsilon_{cc} = 15.0$, (c) $\epsilon_{cc} = 20.0$, and configurations with MCs at: (d) $\epsilon_{cc} = 10.0$, (e) $\epsilon_{cc} = 15.0$, (f) $\epsilon_{cc} = 20.0$.